JOURNAL OF GEOPHYSICAL RESEARCH, VOL. 106, NO. D24, PAGES 33,743–33,754, DECEMBER 27, 2001

Elevation change of the southern Greenland ice sheet from 1978 to 1988: Interpretation

C. H. Davis,[1] J. R. McConnell,[2] J. Bolzan,[3] J. L. Bamber,[4] R. H. Thomas,[5] and E. Mosley-Thompson[6]

Abstract. The spatial pattern of elevation change estimates derived from satellite radar altimeter data for the period from 1978 to 1988 for the southern Greenland ice sheet is examined. As reported previously, the results from 12 ice cores widely distributed in the study area indicate that much of the spatial variability in the elevation change estimates can be explained by temporal variations in accumulation. Most notably, the areas of largest thickening and thinning, east and west of the ice divide around 66°N, recently experienced substantial decadal fluctuations in accumulation sufficient to explain the observed elevation change rates that span the range of ±24 cm yr^{-1}. Elevation change estimates in the NW of the study area around the 2000-m elevation contour were found to be inconsistent with both short- and long-term changes in accumulation fluctuations. Examination of stratigraphy in several shallow ice cores in the NW indicates that significant melting took place in 1977 and 1978, and this was followed by many years of very little melt activity. This likely resulted in a significant downward bias in the 1978-1988 elevation change estimates in the NW. Comparison of measured surface velocities with those calculated assuming steady state balance show very good agreement overall, but there are many instances in the southeast where the steady state velocities are significantly smaller than measured surface velocities. We cannot rule out the possibility that increased ice flow in lower-elevation outlet glaciers has migrated farther upstream thereby causing negative long-term mass imbalance in southeast Greenland.

1. Introduction

Since its inception a key objective of the Program for Arctic Regional Climate Assessment (PARCA) has been the direct measurement of ice sheet elevation change from time series of satellite radar and aircraft laser altimeter data [*Thomas and the PARCA Investigators*, this issue]. After correction for isostatic rebound, surface elevation change measurements of an ice sheet from continuous and/or repeat altimeter surveys are a direct measure of net volume change of the ice sheet. These measurements are important for assessing the current state of the ice sheet and for determining the corresponding impact on sea level change. Aircraft laser altimeter surveys of southern Greenland in 1993 and 1998, and northern Greenland in 1994 and 1999, have provided a comprehensive assessment of elevation change over these 5-year time periods [*Krabill et al.*, 1999, 2000]. Results from the laser surveys, as well as those from volume-balance calculations [*Thomas et al.*, 2000; *Thomas et al.*, this issue], indicate that the upper elevations of the Greenland ice sheet are approximately in a state of balance. In contrast, many of the coastal regions are experiencing rapid and dramatic thinning in excess of 1 m yr^{-1} [*Krabill et al.*, 1999, 2000; *Abdalati et al.*, this issue]. The aircraft laser altimeter measurements provide an important baseline data set for comparison with surface elevations from NASA's Geoscience Laser Altimeter System (GLAS) aboard ICESAT, which is planned for launch in late 2001.

Satellite radar altimeters were developed in the early 1970s with the primary motivation being the study of the world's oceans [*Davis*, 1992]. NASA's Seasat radar altimeter, which operated from July 6 to October 10 in 1978 and then failed, achieved a range precision of 10 cm from an orbiting altitude of 800 km. The Seasat altimeter served as the model for the design of the U.S. Navy's Geosat radar altimeter (1985-1989) and the European Space Agency's ERS-1 altimeter (1991-1997). Even though early spaceborne radar altimeters were primarily designed for oceanographic applications, the orbits of Seasat and Geosat extended to latitudes of ±72.1°, covering major portions of Greenland and Antarctica. Radar altimeters aboard the ERS-1 and ERS-2 satellites have extended coverage of the ice sheets to ±81.5° and provided a nearly continuous time series of data since 1991.

Zwally et al. [1989] were the first to use satellite altimeters for detection of ice sheet elevation change. This study used data from the Seasat and Geosat satellites and concluded that

[1]Department of Electrical Engineering, University of Missouri-Columbia, Columbia, Missouri.
[2]Desert Research Institute, University and Community College System of Nevada, Reno, Nevada.
[3]Columbus, Ohio.
[4]Bristol Glaciology Centre, School of Geographical Sciences, University of Bristol, University Road, Bristol, England, United Kingdom.
[5]EG&G Services, NASA Wallops Flight Facility, Wallops Island, Virginia.
[6]Byrd Polar Research Center and Department of Geography,Ohio State University, Columbus, Ohio.

Paper number 2001JD900167.
0148-0227/01/2001JD900167$09.00

the southern portion of the Greenland ice sheet grew at an average rate of 23 ± 6 cm yr^{-1} from 1978 to 1986. *Zwally* [1989] interpreted this result as evidence of increased precipitation caused by a warmer polar climate. However, these early ice sheet change studies using Seasat and Geosat altimeter data suffered from a variety of problems [*Douglas et al.*, 1990; *Davis*, 1995; *Davis et al.*, 1998]. Progressive improvement in data processing techniques and in our knowledge of satellite orbits and orbit errors has subsequently yielded more accurate estimates of ice sheet elevation change from satellite radar altimeters. Improvements in orbit computation [*Tapley et al.*, 1996], orbit-error analysis and reduction [*Yoon*, 1998; *Davis et al.*, 2000], ice sheet retracking methods [*Davis*, 1997], and identification of measurement system biases have been incorporated in more recent elevation change estimates derived from the historical Seasat and Geosat altimeter data sets [*Davis et al.*, 1998; 2000]. Ice sheet satellite radar altimetry has evolved to a sufficient state of maturity that regional changes in surface elevation can now be inferred with an accuracy on the order of a few centimeters per year over periods of 5-10 years [*Davis et al.*, 1998; *Wingham et al.*, 1998; *Davis et al.*, 2000].

Recent reexamination of the historical Seasat and Geosat altimeter data sets found that the average elevation change of the southern Greenland ice sheet from 1978-1988 for elevations above 2000 m was not significantly different from zero [*Davis et al.*, 1998, 2000]. These results have been independently confirmed by the airborne laser altimeter results from 1993 to 1998 [*Krabill et al.*, 1999]. In addition, the spatial pattern of elevation change from the 1978-1988 radar altimeter and 1993-1998 laser altimeter surveys were found to be in qualitative agreement over large areas of the southern ice sheet [*Krabill et al.*, 1999; *Davis et al.*, 2000]. A more detailed and quantitative comparison of the elevation change results from the radar and laser altimeter studies is given by *Thomas et al.* [1999].

While the average rate of elevation change for the southern Greenland ice sheet above 2000 m is essentially zero, the radar altimeter results revealed regional variations in the elevation change estimates from –24 to +24 cm yr^{-1} over distances as small as only 200 km. A large volume of in situ data has been collected as a result of the PARCA program that can further our understanding of the observed elevation change estimates. In this paper, we examine the spatial pattern of the 1978-1988 satellite radar altimeter elevation change estimates using various in situ data sets to help understand their cause. In section 2 we give a brief summary of the latest radar elevation change map and then compare this updated map with elevation change results from other studies. In section 3 we examine the spatial and temporal variability in snow accumulation to determine their influence, if any, on the observed radar elevation change results. In section 4 we investigate a possible temporal change in near-surface snow characteristics to understand differences between radar and laser altimeter elevation change results in one region of the study area. Finally, in section 5 we compare measured surface velocities with estimated balance velocities to determine possible contributions of long-term ice flow to the observed radar elevation change results. These analyses are important for determining whether or not the observed radar altimeter elevation changes are due to short- or long-term changes in the major processes that drive ice sheet mass balance (accumulation, ice flow, etc.).

2. Spatial Pattern of Elevation Change

Plate 1 shows a map of the spatial distribution of the rate of elevation change (*dH/dt*) from 1978 to 1988 for southern Greenland (< 72.1°N) derived from an analysis of Seasat (July 6 to October 10, 1978) and Geosat (April 1985 to November 1988) satellite radar altimeter data. Also shown on the map are the 2000-m surface elevation contour, the ice divide, and the locations of nine shallow and three deeper ice cores in the study area. The technical details of the major procedures used in generating the radar *dH/dt* map are given by *Davis et al.* [2000]. However, two small changes in these procedures have slightly altered the version given in Plate 1 compared to the previously published version. First, the average elevation change estimate for each 50 x 50 km grid cell was computed after excluding individual elevation change measurements that exceeded 2 standard deviations from the primary Gaussian distribution (2 SD edit). This reduced the spatial variability of the *dH/dt* estimates between adjacent cells in a few areas where there were small numbers of measurements within a given cell. This did not alter any of the regional patterns of elevation change evident in Plate 1 but only served to improve the spatial coherence of the elevation change estimates from cell to cell within certain regions.

In addition, we excluded *dH/dt* estimates for a given cell when the random error estimate (i.e., from sampling variability) exceeded ±4 cm yr^{-1} after the 2 SD edit. This eliminated only five *dH/dt* cells found in the map previously published by *Davis et al.* [2000]. The number of elevation change estimates within a given cell varies considerably with elevation and latitude, with more measurements at higher elevations and latitudes. While an average *dH/dt* estimate is calculated with as few as 10 measurements in a cell [*Davis et al.*, 2000], the median value is 180 measurements. Less than 10% of the 170 *dH/dt* grid cells in Plate 1 had random error estimates that exceeded ±2 cm yr^{-1}, and the median random error in the cells was ±0.4 cm yr^{-1}. In addition to the random measurement error, uncertainties in various corrections applied to the elevation data contribute about ±1-2 cm yr^{-1} to the total error budget [*Davis et al.*, 1998, 2000]. Considering all error sources, a typical error value for elevation change estimates in a 50 x 50 km cell is approximately ±2 cm yr^{-1}.

The elevation change results in Plate 1 cover an area of 425,000 km^2, located largely above the 2000-m contour. About 75% of the area between 1700 m and 2000 m is covered for the area west of the ice divide, while no coverage below 2000 m is available east of the ice divide. No coverage is available for the lower elevations of the ice sheet because of the poor quality, limited quantity, and poor spatial distribution of the Seasat-Geosat elevation change measurements [*Davis et al.*, 2000]. After isostatic adjustment the average rate of elevation change for the entire area is +1.0 cm yr^{-1}. For a total error budget on the order of ±1-2 cm yr^{-1} [*Davis et al.*, 2000], this result is not significantly different than zero or significantly different than the earlier published estimates given by *Davis et al.* [1998, 2000].

The upper elevations between 70° and 72° N and immediately south of Summit station (72.3°N, 322°E) show close to zero change. This is in very good agreement with a mass balance estimate of 1 ± 3 cm yr^{-1} for the Summit area derived from accumulation estimates at nine shallow cores and GPS surface velocity measurements [*Bolzan*, 1992].

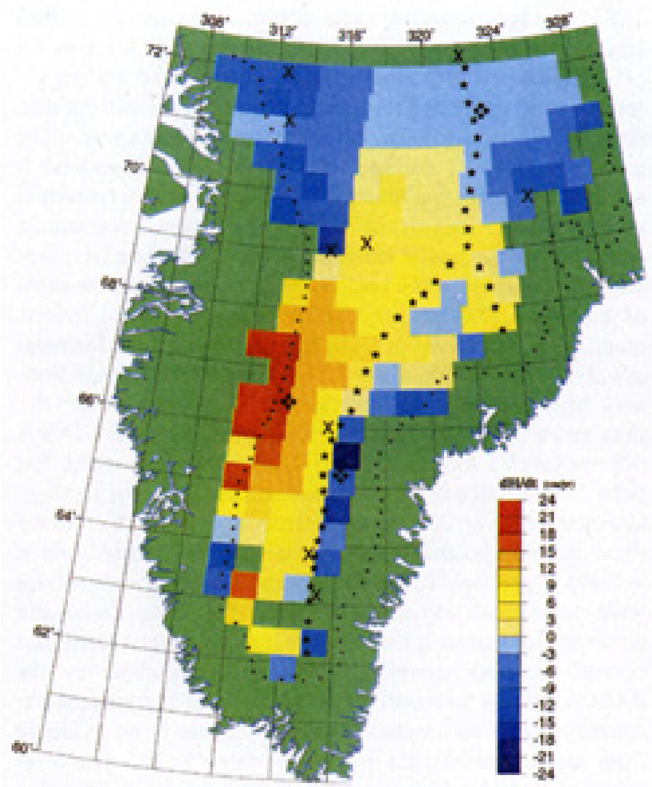

Plate 1. Spatial distribution of elevation change from 1978 to 1988 from an analysis of Seasat and Geosat altimeter data (adapted from *Davis et al.* [2000]). The approximate location of the ice divide (stars), 2000-m surface elevation contour (dots), nine shallow ice cores (crosses), and three deeper ice cores (diamond clusters) are also shown.

Thinning is indicated for the lower elevations immediately east and west of the Summit area, with stronger thinning (approximately −10 cm yr^{-1}) for much of the area near the 2000-m contour in the west. For the area immediately west of the ice divide from 66° to 72°N, there is a gradient ranging from strong positive elevation change (>15 cm yr^{-1}) at 66°N to essentially zero change north of 70°N. There are alternating regions of small thinning and modest thickening east of the ice divide between 67° and 70°N. The local ice dome in the east around 68° to 69°N has the largest growth rates (~8 cm yr^{-1}) of any region east of the ice divide in the study area.

The largest elevation changes occur in the region from 64° to 68°N on both sides of the ice divide. In the west the area along the 2000-m contour from 66° to 68°N has strong growth with *dH/dt* estimates on the order of +20 cm yr^{-1}. There is a clear and spatially coherent decrease in the *dH/dt* estimates as one moves eastward from this area to higher elevations and the ice divide. There is a strong *dH/dt* gradient starting at the Dye 2 station (66.4°N, 313.8°E) and heading SE toward the Dye 3 station (65.2°N, 316.1°E) where the *dH/dt* estimates change from +24 cm yr^{-1} to −24 cm yr^{-1} over a distance of less than 200 km. Finally, there is an abrupt transition from positive to negative elevation change from west to east that coincides with the location of the ice divide for the latitudes from 62° to 66°N. In this area, the *dH/dt* values along the western slope and immediately adjacent to the ice divide are typically +6 to +9 cm yr^{-1}, while along the eastern slope of the ice divide there is substantial variation between −5 and −24 cm yr^{-1}.

The same spatial pattern of thickening in the west and thinning in the east after crossing the ice divide is evident in the elevation change map from the airborne laser altimeter survey from 1993 to 1998 [*Krabill et al.*, 1999]. It has also been observed in TOPEX/Poseidon radar altimeter data south of 66°N for the time period from 1991 to 1997 [*Legresy et al.*, 2000]. During the summer of 1980 a series of 22 stations were established near 65°N [*Drew*, 1983]. The stations start in the area around the 2000-m contour in the west and extend past the ice divide all the way to the 2500-m contour in the east. The elevations of these stations were obtained from a satellite Doppler geoceiver (geodetic receiver) survey in 1980. The same stations were resurveyed by airborne laser altimeter in 1993 and 1994, and the corresponding 1980-1993/1994 elevation change results for these stations, first reported by *Krabill et al.* [1995], show the same W-E gradient of positive to negative elevation change. Since the geoceiver-laser *dH/dt* estimates overlap a significant period of the 1978-1988 radar *dH/dt* results in Plate 1, a comparison was made to determine the level of agreement/disagreement. Four clusters (A, B, C, and D) of stations were formed from west (A) to east (D). Radar *dH/dt* values were computed within a radius (nominally 30 km) centered on the central location of each cluster group [*Thomas et al.*, 1999]. The comparison results are summarized in Table 1. The results are in excellent agreement, and this independently confirms the strong W-E gradient seen in the radar *dH/dt* map around 65°N. This effectively demonstrates that the satellite radar *dH/dt*

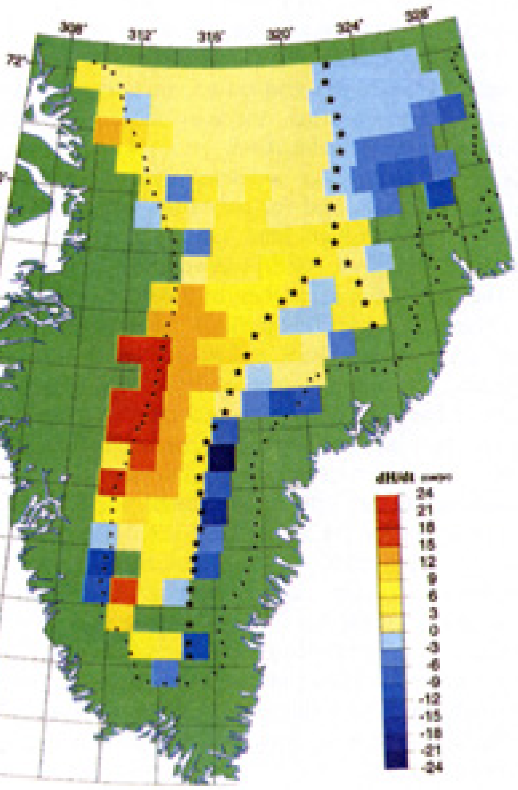

Plate 2. Altered version of the radar *dH/dt* map shown in Plate 1 where many of the elevation change estimates in the NW have been corrected using the regression shown in Figure 5.

Table 1. Comparison of Elevation Change Estimates From Radar and Laser Surveys[a]

Cluster	Central Location	1978-1988 Radar dH/dt, cm yr^{-1}	1980-1993/1994 Laser dH/dt, cm yr^{-1}
A	65.4°N, 312.3°E	13.1 ± 2.6	14.2 ± 4.0
B	65.1°N, 314.3°E	11.9 ± 2.6	9.4 ± 4.0
C	65.0°N, 315.6°E	-1.5 ± 1.8	-1.0 ± 4.0
D	65.2°N, 316.3°E	-10.6 ± 2.2	-9.0 ± 4.0

[a]Adapted from *Thomas et al.* [1999].

estimates, derived from the historical Seasat and Geosat altimeter data sets, can accurately characterize *dH/dt* variations over regions as small as 2500 km^2 with errors of approximately ±2.5 cm yr^{-1}.

3. Spatial and Temporal Accumulation Variability

Snow precipitation/accumulation is one important process that can affect surface elevation change, and therefore ice sheet mass balance, over interannual, decadal, and even century timescales. Recent analysis of PARCA and European firn and ice cores have doubled the number of years in accumulation records from the Greenland ice sheet and have yielded more accurate spatial estimates of snow accumulation [*Bales et al.*, 2001; *Mosley-Thompson et al.*, this issue]. We examined the spatial correlation scale of the improved accumulation estimates in comparison to the 1978-1988 radar and 1993-1998 laser elevation change estimates in southern Greenland. A 20-km gridded accumulation map from *Bales et al.* [2001] was used, and only those accumulation data falling within the radar *dH/dt* cells (Plate 1) were selected. For the airborne laser altimeter data, average laser *dH/dt* values were computed for only those radar *dH/dt* cells that contained aircraft flight lines (i.e., the interpolated laser *dH/dt* map of *Krabill et al.* [1999] was not used).

The spatial autocorrelation of the three data sets is shown in Figure 1. For a 50% threshold the correlation scale for the laser *dH/dt*, radar *dH/dt*, and accumulation data are 75 km, 110 km, and 160 km, respectively. The larger correlation scale of the radar *dH/dt* data relative to the laser *dH/dt* data for the study area is likely due to the longer time period of the radar *dH/dt* observations. Interannual variations in accumulation are likely to cause more rapid spatial decorrelation for the 5-year laser *dH/dt* estimates relative to the 10-year radar *dH/dt* estimates. The improved accumulation map is representative of the average accumulation over the last several decades (1970s-1990s) [*Bales et al.*, 2001]. However, it was produced from kriging of accumulation values measured from ice core sites that are unevenly distributed throughout the study area. Thus it is difficult to determine how well the correlation function in Figure 1 represents the spatial correlation of the actual accumulation field. Note that *Bales et al.* [2001] used a range of 200 km in a spherical semivariogram model for kriging, so the 160-km correlation scale represents an upper limit for the study area.

For the accumulation, radar *dH/dt*, and laser *dH/dt* data sets the 1 standard deviation (SD) spatial variability was 8.8 cm yr^{-1} (water equivalent (we)), 9.0 cm yr^{-1}, and 8.5 cm yr^{-1} respectively. Note that the accumulation and laser *dH/dt* data sets are subsets of the overall data as described above. The average density of the snowpack in southern Greenland is around 0.5 g/cm^3 for a time period of 20-30 years [*Thomas et al.*, this issue]. Thus, if the longer-term accumulation pattern were causing the spatial variability in the *dH/dt* data sets, then one would expect to see spatial *dH/dt* variability on the order of 8.8/0.5 = 17.6 cm yr^{-1}, which is not the case. Indeed, qualitative comparison between the spatial pattern in the radar *dH/dt* map and the improved PARCA accumulation map finds very little resemblance. Cross correlation between the two data sets yielded a correlation coefficient of –0.15. This is not unexpected for an ice sheet in mass balance, which has been demonstrated by four independent estimates for southern Greenland above ~2000 m [*Thomas et al.*, this issue]. An ice sheet in mass balance is one where the downward surface velocity is precisely balanced by snow accumulation. If there were substantial correlation between the radar *dH/dt* and accumulation patterns, this would suggest that the recent (last several decades) accumulation pattern represented by the PARCA map is substantially different from the longer-term (century scale) accumulation pattern. There is no evidence from three intermediate-depth ice cores (>200 years) in southern Greenland, discussed later, that would suggest that this is the case.

Temporal, rather than spatial, variations in accumulation rate are likely to have greater impact on elevation change estimates from repeat altimeter surveys over 5- to 10-year time periods. *van der Veen* [1993] demonstrated that random interannual fluctuations in accumulation can produce large changes in surface elevation over decadal timescales. Nine shallow cores and three deeper cores, widely distributed over the study area (Plate 1), covered at least the time period from 1978 to 1988. Annual accumulation records reconstructed from these cores can be used to assess the effect of interannual accumulation variability on the radar *dH/dt* estimates. *McConnell et al.* [2000] used the annual accumulation records at these 12 sites in conjunction with a physical model of snow densification [*Arthern and Wingham*, 1998] to derive elevation change estimates due solely to the measured accumulation variability. These were then compared with radar *dH/dt* estimates that were an average of

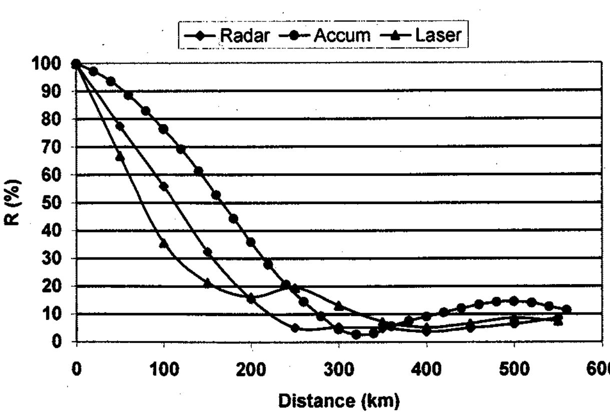

Figure 1. Spatial autocorrelation of accumulation, laser, and radar dH/dt estimates for the southern Greenland study area.

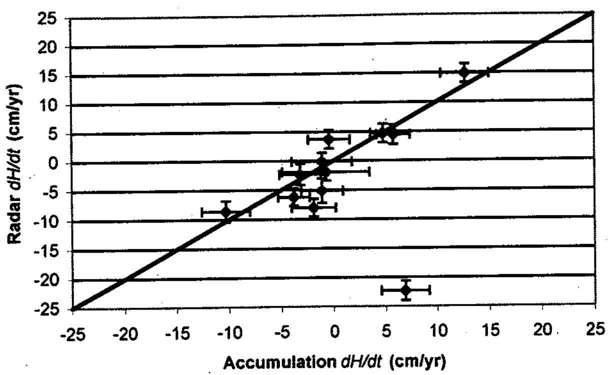

Figure 2. Scatterplot of radar elevation change estimates and corresponding elevation change estimates due solely to short-term fluctuations in accumulation at 12 ice core locations in the study area [*McConnell et al.*, 2000].

all elevation change measurements within a circular area centered on the ice core location. A nominal radius of 20 km was used for 10 of the core sites, while a radius of 30 km was used for two core locations (Summit and Dye 3). A 2 SD edit was used on each set of radar elevation change measurements to eliminate data outliers. A scatterplot of the radar and accumulation *dH/dt* estimates is shown in Figure 2 [*McConnell et al.*, 2000]. A 0.5-cm yr^{-1}correction for isostatic rebound was applied to the radar *dH/dt* estimates. The error bars for the radar *dH/dt* estimates are shown as ±1 SD and take into account random error as well as uncertainties in various corrections applied to the elevation data [*Davis et al.*, 2000]. The error bars for the accumulation *dH/dt* estimates are shown as ±1 SD and include estimates for the model uncertainties, short-scale spatial variability of the accumulation rate, and uncertainties in the accumulation history prior to the beginning of the core record [*McConnell et al.*, 2000].

The accumulation and radar *dH/dt* estimates agree to within 1 SD for 9 of the 12 core sites [see *McConnell et al.*, 2000, Table 1]. At these 9 core locations the accumulation and radar *dH/dt* estimates vary over a range from −10 to +15 cm yr^{-1}. Most importantly, the accumulation *dH/dt* estimates capture the change in the radar *dH/dt* map from strong thickening in the vicinity of Dye 2 (66.4°N, 313.8°E) to moderate thickening just west of the ice divide (66°N, 315.5°E), to strong thinning just beyond the ice divide at Dye 3 (65.2°N, 316.1°E). This strongly suggests that the area from 65° to 67° N, which contains the radar *dH/dt* estimates with the largest thickening and thinning rates, is responding primarily to temporal changes in accumulation over the 10-year period from 1978 to 1988. The extreme outlier in Figure 2 occurs at the core located at 69.0°N, 315°E in the NW of the study area, and a possible reason for this strong disagreement will be discussed in detail in section 4.

It is fortuitous that deeper ice cores are available at Dye 2 and Dye 3 in the area where the greatest spatial variability is observed in the radar *dH/dt* map. This allows us to examine the decadal variability in accumulation over the last century and beyond at these locations. We examined the Dye 2 and Dye 3 accumulation histories over the time periods from 1801 to 1997 and from 1770 to 1987, respectively. The third deeper ice core in the study area is located at Crete station (71.1°N, 322.7°E), and the accumulation history for this analysis covers the period from 1778 to 1989. The accumulation records at the three deeper core sites are a compilation of both previously reported and new PARCA cores as described by *McConnell et al.* [2000]. The Crete station is in an area where the combined radar and laser *dH/dt* estimates indicate essentially zero change over the last two decades, and this is in agreement with a mass balance estimate based on ice volume input versus output calculations [*Bolzan*, 1992]. In addition, it is located at a much higher latitude and elevation compared to the Dye 2 and Dye 3 cores. For each of the deep cores we computed the average accumulation rate for the twentieth century and for each available decade in the twentieth century (note that each decade average was formed using years *X*0-*X*9). Partial decade averages for Dye 2 and Dye 3, each containing 8 years (e.g., 0-7), were computed for the incomplete decades at the end of these two cores.

A plot of the percentage difference of each decade's average accumulation with respect to the twentieth-century average is shown for the three deep cores in Figure 3. Prior to 1960, the decadal difference from the century average was largely in the range of ±10% for both the Dye 2 and Dye 3 cores. Since 1960, there have been several decades where the average accumulation at Dye 2 or Dye 3 was more than ±20% different than the century average. At Dye 2 the 1960s and 1970s were decades where the average accumulation was more than 20% below the century average. This was followed by decades of significantly higher than normal accumulation in the 1980s (+12%) and 1990s (+37%). The average accumulation rate at Dye 2 for the twentieth century is 33.7 cm yr^{-1} we. Assuming an average near-surface snow density of 0.45 g cm^{-3} for a 10-year period [*Thomas et al.*, this issue], a 35% increase in accumulation over a 10-year period, as occurred between the 1970s and 1980s at Dye 2, is sufficient to cause elevation increases on the order of +25 cm yr^{-1} (ignoring the effect of density fluctuations). Since the radar *dH/dt* estimates span the period from 1978 to 1988, the strong thickening west of the ice divide in the vicinity of Dye 2 is entirely consistent with the abrupt change from strongly below average accumulation in the 1960s and 1970s to above average accumulation in the 1980s.

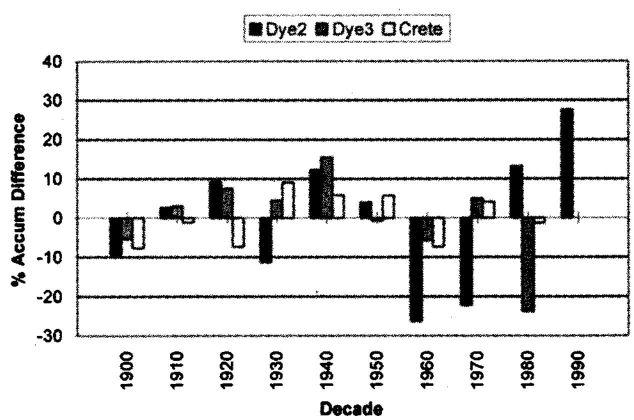

Figure 3. Percent difference between decadal averages of snow accumulation and the long-term average since 1900 at three deeper core locations in the study area (see Plate 1). Note the large differences at Dye 2 from the 1960s to 1990s and at Dye 3 in the 1980s.

Table 2. Percent Variability From Long-Term Average Accumulation Rate for Various Time Intervals[a]

Site	Location °N / °E	Time Period	Elevation, m	Average Accumulation, cm yr^{-1} we: Since 1900	Average Accumulation, cm yr^{-1} we: Since Initial Year	Variability in Twentieth Century, %: 1 year	Variability in Twentieth Century, %: 5 years	Variability in Twentieth Century, %: 10 years	Variability Since Initial Year in Core, %: 1 year	Variability Since Initial Year in Core, %: 5 years	Variability Since Initial Year in Core, %: 10 years	Variability Since Initial Year in Core, %: 20 years
Dye 2	66.4 / 313.8	1801-1997	2053	33.7	33.0	33	20	19	33	18	16	14
Dye 3	65.2 / 316.1	1770-1987	2477	52.6	48.6	24	13	11	26	15	13	11
Crete	71.1 / 322.7	1778-1989	3174	25.1	24.5	17	8	7	18	9	6	5

[a]Calculated as ratio of 1 standard deviation variability to long-term average accumulation.

At Dye 3 the 1960s and 1970s were decades where the average accumulation was only slightly above or below the century average (-6% in the 1960s and +5% in the 1970s). However, in the 1980s the average accumulation rate was 24% below the century average. The average accumulation rate at Dye 3 for the twentieth century is 52.6 cm yr^{-1} we. Following similar arguments, the nearly 30% decrease in accumulation from the 1970s to the 1980s could cause elevation changes on the order of –35 cm yr^{-1} (ignoring density fluctuations). Thus it is also entirely reasonable that the strongly below-average accumulation experienced in the 1980s at Dye 3 is sufficient to explain the strongly negative radar elevation change estimates east of the ice divide around 65°N.

At Crete station the effect of decadal fluctuations in accumulation is minimal. Nearly all the decadal differences from the twentieth-century average fall within the range of ±7%. For the 1970s and 1980s, the decadal averages differ from the century average by only +4% and –1% respectively. The average accumulation rate for the twentieth century at Crete is 25.1 cm yr^{-1} we. Following the same calculations as in the preceding paragraphs, a 5% decadal change in accumulation will affect 10-year elevation change estimates at a level of about ±2.5 cm yr^{-1}, which is comparable to the error budget for both the radar and laser dH/dt estimates.

The discussion above focused on decadal variability in accumulation at the Dye 2, Dye 3, and Crete stations because of the 10-year time period for the radar dH/dt estimates. It is also useful to consider other time intervals because of the various time spans of other elevation change estimates. Table 2 summarizes the accumulation variability at different time intervals (1 year, 5 years, etc.) for the twentieth century and for the entire history available in the particular record at each site. Also shown are the average accumulation values for the twentieth century and the entire record. The percent variability is calculated as the ratio of 1 SD to the average accumulation over the period of interest (twentieth century or entire history). There has been an 8% increase in the average accumulation rate at Dye 3 for the twentieth century relative to the average for the complete record. At Dye 2 and Crete there have been very small (~2%) increases which are probably insignificant. The twentieth-century variability estimates agree with those from the complete record at each site for the various time intervals to within 2%. Thus the variability this century is consistent with that in the longer-term record.

The results show that, at least for this limited number of cores in southern Greenland, the variability is dependent upon elevation, with significant decreases in the variability with increasing elevation. Note that even though the average accumulation rate at Dye 3 is 50% greater than that at Dye 2, the variability estimates are significantly smaller than those at Dye 2. In assessing the uncertainty in regional and ice sheet wide elevation change estimates in Antarctica due to accumulation fluctuations over a 5-year time period, *Wingham et al.* [1998] assumed the accumulation variability was a fixed percentage of the average accumulation rate. The results in Table 2 suggest that the accumulation variability is spatially variable and dependent upon elevation, at least in southern Greenland. In addition to elevation, other factors such as latitude and proximity to the ocean may also affect the magnitude of the accumulation variability. Thus we feel it would be beneficial as more core data are analyzed to attempt to model and/or understand the spatial dependence of the accumulation variability for the entire ice sheet. This is important for determining at what level and over what length of time observed elevation change estimates for an entire ice sheet would have to be in order to be significantly different than what could be explained by accumulation variability.

The interannual variability values in Table 2 range from 18 to 33% for the complete records at the three deeper core sites. These are only point estimates of the interannual variability, and as such, these should be greater than the interannual variability averaged over larger areas. *McConnell et al.* [this issue] used ice core measurements of accumulation to develop maps of net annual accumulation over southern Greenland from 1975 to 1998. Results indicate that the net accumulation, when integrated over the southern ice sheet (< 73°N) above the 2000-m elevation contour, has an interannual variability of 11%.

Finally, the results in Table 2 show that, at least for these three deeper cores in southern Greenland, there are only small reductions in the accumulation variability for time periods beyond 5 years. Typically, reductions of only 2% occur in the variability estimates when the time interval increases from 5 to 10 years and then from 10 to 20 years. Thus, from the perspective of statistical reduction in accumulation variability, there is only modest benefit in developing elevation change estimates over periods >5-10 years. However, the results above and those of *McConnell et al.* [2000] demonstrate that the strong thickening and thinning observed in the radar dH/dt estimates from 1978 to 1988 around 66°N can be explained by long-period (>10 years) changes in accumulation. We believe that accumulation should not be treated as a random variable for periods less than at least 20 years and possibly longer (note the strong trend of increasing accumulation at Dye 2 over the last 40 years in Figure 3). Rather, accumulation should be measured and/or modeled for the time period of interest to determine the impact of accumulation variability on elevation change estimates based on time series spanning <20 years.

4. Temporal Change in Near-Surface Snow Conditions

For the comparison between the radar *dH/dt* estimates and those predicted from short-term temporal variability in snow accumulation (Figure 2), the greatest discrepancy occurred for the shallow core located at 69°N, 315°E near the 2000-m contour. At this location the radar *dH/dt* estimate was –22.3 ± 1.7 cm yr^{-1} compared to an accumulation *dH/dt* estimate of +6.9 ± 2.3 cm yr^{-1}, or a difference (accumulation minus radar) of nearly +30 cm yr^{-1}. At a nearby ice core (69.2° N, 317° E), only 80 km away but at a higher elevation, the radar and accumulation *dH/dt* estimates were +4.5 ± 1.7 cm yr^{-1} and +5.8 ± 1.6 cm yr^{-1}, respectively, and therefore were in very good agreement. Farther north, but also near the 2000-m elevation contour, the accumulation *dH/dt* estimates at 71.1°N, 312.8°E and 71.9°N, 312.5°E differed from the radar *dH/dt* estimates by +4 and +6 cm yr^{-1}, respectively. Excluding the three ice cores in the NW closest to the 2000-m contour, the average absolute difference between the accumulation and radar *dH/dt* estimates at the nine other core locations was only 1.7 cm yr^{-1}.

The difference between the accumulation and radar *dH/dt* estimates that occur in the NW near the 2000-m contour could be a case of the radar *dH/dt* estimates reflecting a long-term elevation change trend rather than a short-term elevation anomaly due to temporal variability in accumulation. However, there are many other pieces of ancillary data and information that lead us to believe that this is not the case. Indeed, the compilation of these other observations indicates that there is good reason to believe that the radar *dH/dt* estimates in this area may be erroneous.

A comparison of the 1978-1988 radar and 1993-1998 laser *dH/dt* estimates in this area shows significant disagreement that cannot be explained by changes in the average accumulation rate during the two time periods [*Thomas et al.*, 1999]. For the area bounded by 70°-72°N, 310°-317°E, the laser *dH/dt* estimates were on average +8 cm yr^{-1} larger than the radar *dH/dt* estimates. In addition, the difference between the radar and laser *dH/dt* results is strongly correlated (inversely) with elevation (see Figure 5). For the two cores located at 71.1°N, 312.8°E and 71.9°N, 312.5°E the difference between the average accumulation rates for the time periods 1978-1988 and 1993-1996 was insignificant (~1%). Farther south near 69°N, 316°E the average accumulation rates at the two nearby cores decreased by ~ 10-15% for the period from 1993-1997 compared to 1978-1988. While the accumulation estimates do not span the entire 5-year period from 1993 to 1998 of the laser *dH/dt* estimates, it is very unlikely that increases in accumulation can account for the significantly larger laser *dH/dt* estimates in this area of the ice sheet. As there is very good agreement between the radar and laser *dH/dt* estimates for other areas of the ice sheet [*Thomas et al.*, 1999] (see also Table 1), the discrepancy between the radar and laser *dH/dt* estimates for the two different time periods indicates that the radar *dH/dt* estimates are not representative of a long-term trend. The fact that the discrepancy cannot be explained by accumulation differences between the two time periods suggests that something may be wrong with one or both sets of the *dH/dt* estimates.

A previous analysis of Seasat and Geosat altimeter waveforms from the Greenland ice sheet found large differences in the scattering properties of the surface and near-surface snow in an area roughly from 70° to 72°N, 317° to 322°E [*Davis*, 1996]. Over regions with surface slopes less than ~0.5°, the average shape of the Seasat/Geosat altimeter waveforms are largely dependent on the geophysical properties of the snow from the surface down to depths up to 10 m [e.g., *Ridley and Partington*, 1988; *Davis and Zwally*, 1993]. In the area indicated above, the study found that the

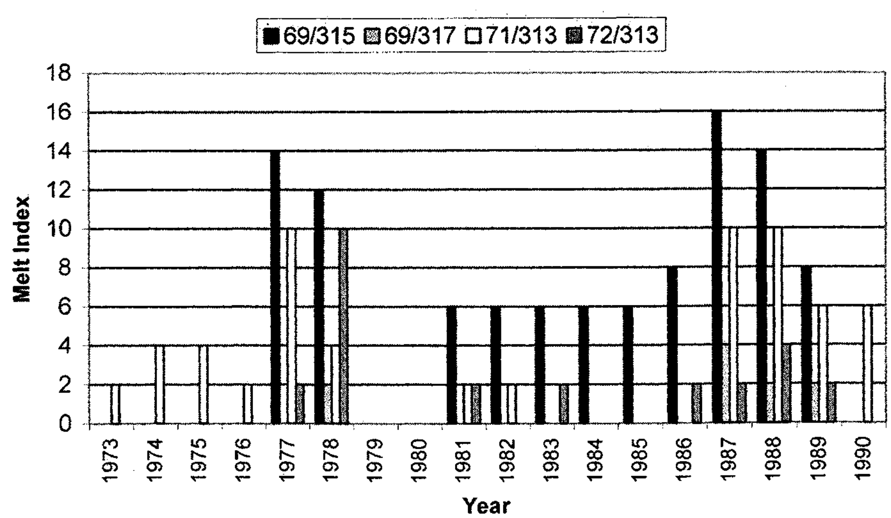

Figure 4. Melt index derived from stratigraphy of four shallow ice cores near the 2000-m elevation contour in the NW of the study area. Note the strong melting in 1977 and 1978 for three of the cores.

Seasat waveforms were dominated by surface scattering, whereas the Geosat waveforms were dominated by subsurface volume scattering. Significant differences were not present at the ice divide and east of the ice divide from 70° to 72°N, and also were not present south of ~69°N. The study was confined to areas with surface slopes <0.25° and therefore did not cover areas west of 317°E and closer to the 2000-m contour in the NW of the present study area.

The *Davis* [1996] study suggested two possible causes to explain the observed differences in the Seasat and Geosat waveforms. The first hypothesis was that there was a significant increase in the accumulation rate in the area during the period from 1978 to the mid-1980s relative to the decade preceding the 1978 Seasat measurements. While this did occur in the Dye 2 area much farther south, the accumulation record from the Crete core and a series of other cores in the Summit area [*Bolzan and Strobel*, 1994] provides no evidence to support this hypothesis. Furthermore, if this had occurred, we would expect to see strongly positive radar *dH/dt* measurements in the NW area, just as occurred in the Dye 2 area. Since this is clearly not the case, we can eliminate this possibility.

The second hypothesis was that there was a large melt event during or immediately preceding the Seasat observations in 1978 [*Davis*, 1996]. This would then have to have been followed by relatively benign (i.e., no melting) conditions in the years leading up to the Geosat measurements in the mid-1980s. This would cause the Seasat waveforms to be dominated by surface scattering because of the presence of liquid water and/or the presence of significant ice layers near the surface from melting and refreezing. Conversely, there would be significant penetration of the altimeter signal during the Geosat time period because of the absence of these features, and this would give rise to waveforms exhibiting volume-scattering characteristics. This would cause the Seasat elevation measurements to be biased higher relative to the Geosat elevation measurements. This, in turn, would cause Geosat-Seasat radar *dH/dt* estimates to be biased downward with respect to the true *dH/dt* trend over the given time period. The magnitude of the downward bias would depend upon the strength of the melting in a given area, and this should be, in general, spatially variable, as the strength of the melting is likely to decrease with increasing elevation and possibly with latitude as well. This could account for the differences observed between the radar and laser *dH/dt* estimates in the NW of the study area.

We examined the core stratigraphy of the four shallow cores located north of 69°N and immediately adjacent to the 2000-m contour. The examination found that many significant melt events, represented by ice layers and ice lenses in the cores, occurred in 1977 and 1978 for the three cores nearest the 2000-m contour, located roughly at 69°N, 315°E; 71°N, 313°E; and 72° N, 312°E, whereas only two occurrences of ice lenses (both in 1978) were seen for the core near 69°N, 317°E. To quantify these events, we calculated a melt index for each year in a given core's record. Each occurrence of ice lenses in the stratigraphy was assigned a value of 1 and each occurrence of an ice layer was assigned a value of 2. The sum for each year was then totaled, and a graph of the melt index for the four cores is shown in Figure 4. The two cores around 69°N spanned the time period from 1977 to 1997, and the two cores around 71°N spanned the time period from 1973 to 1996. The results show that melting

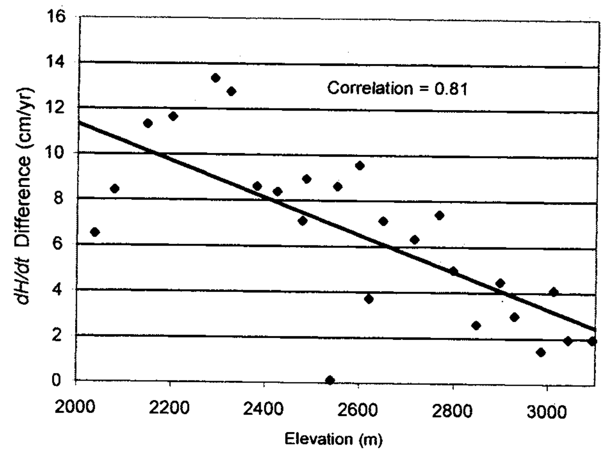

Figure 5. Difference between radar and laser elevation change estimates in the NW of the study area. Note the strong correlation of the difference with elevation.

in the years following the strong melt years of 1977 and 1978 was relatively benign up until 1987.

We examined the average monthly temperature record at the nearby Jakobshavn coastal station [*Frich et al.*, 1996]. The month of July normally had the maximum average air temperature in a given year. The temperature data show that the largest summer temperatures for the 2 decades from 1970 to 1990 occurred in the years 1977 and 1978. The 1977 and 1978 summers were typically 2°C warmer, on average, than the summers from 1978 to 1986. This strongly supports the observations found in the core stratigraphy. A similar 1977-1978 maximum was not found in temperature records south of Jakobshavn. Thus it would appear that the 1977 and 1978 warming was confined to only this region of southern Greenland.

The Geosat data used to produce the radar *dH/dt* map in Plate 1 spanned the time from April 1985 to November 1988. Roughly 75% of the Geosat-Seasat elevation change measurements in the NW area of the ice sheet preceded the summer of 1987. Thus it is very likely that the elevation change estimates in this area have been biased downward because of the substantial melting that took place in years 1977 and 1978. The results corresponding to the two cores near 69°N are particularly convincing. The stratigraphy for the 69°N, 315°E core shows strong melting in both 1977 and 1978. The corresponding radar *dH/dt* estimate (centered on the core location) is –22 cm yr^{-1}, and this is in strong disagreement with the *dH/dt* estimate of +7 cm yr^{-1} predicted by accumulation variability for 1978-1988 [*McConnell et al.*, 2000]. Conversely, the stratigraphy for the 69°N, 317°E core shows no melting in 1977 and very little melting in 1978. The corresponding radar *dH/dt* estimate (centered on the core location) is +5 cm yr^{-1}, and this is in very good agreement with the *dH/dt* estimate of +6 cm yr^{-1} predicted by accumulation variability for 1978-1988 [*McConnell et al.*, 2000]. Note also that the discontinuity in the radar *dH/dt* map, bounded by the two core locations at 69°N, continues northward, but the magnitude of the difference across the discontinuity decreases with increasing latitude and distance from the 2000-m contour, which is what one would expect if melting were corrupting the radar *dH/dt* estimates in the lower elevations.

Thus we believe there is compelling evidence from a variety of independent sources and studies that, when analyzed in total, strongly indicates that many of the radar *dH/dt* estimates in the NW of the study area have been biased downward because of differences in the surface conditions resulting from strong melt years in 1977 and 1978. Figure 5 shows a scatterplot of the difference between the 1993-1998 laser and 1978-1988 radar *dH/dt* estimates (laser minus radar) as a function of elevation. Radar *dH/dt* cells north of 70.5°N and west of 322°E were used in the regression along with radar *dH/dt* cells west of 316.5°E and between 69.5° and 70.5° N (i.e., west of the radar *dH/dt* discontinuity). These are the areas where we feel there is sufficient evidence to support our contention that the radar *dH/dt* estimates are erroneous. All *dH/dt* values in these two areas were corrected using the average elevation within each radar *dH/dt* cell and the linear regression from Figure 5. The resulting corrected radar *dH/dt* map is shown in Plate 2, where the negative radar *dH/dt* estimates in the NW are now, for the most part, slightly positive. We have no way of developing rigorous estimates for the uncertainty in the radar *dH/dt* estimates that have been corrected as outlined above. We can only say that we feel these are more representative of the real *dH/dt* trend over the period from 1978 to 1988 than the uncorrected values in the two areas delineated above. After correcting for isostatic rebound, a spatial average of the corrected radar *dH/dt* map in Plate 2 yields an average growth rate of +2.7 cm yr^{-1} compared to +1.0 cm yr^{-1} for the version in Plate 1.

5. Ice Flow

The results from many different recent studies all indicate that the upper elevations of the southern Greenland ice sheet are very close to a state of mass balance [*Davis et al.*, 1998; *Krabill et al.*, 1999; *Thomas et al.*, 2000, this issue]. The results from *McConnell et al.* [2000] and those in section 3 provide important evidence that demonstrates that the areas undergoing the strongest change in the radar *dH/dt* estimates, both positive and negative, can be reasonably explained by temporal variations in accumulation over the period from 1978 to 1988. Thus it would appear that there are no regions represented in Plates 1 and 2 that represent areas with significant long-term mass imbalance.

Nevertheless, we feel it is important to briefly examine the potential impact of increased ice flow velocities as it pertains to the radar *dH/dt* estimates in southeast Greenland (south of 67°N and east of the ice divide). The laser altimeter *dH/dt* estimates for 1993-1998 have the same abrupt transition from positive to negative elevation change at the ice divide south of 67°N [*Krabill et al.*, 1999]. More importantly, the laser *dH/dt* estimates found that the thinning in the upper elevations extended all the way to the coastal outlet glaciers where the thinning rates exceeded 2 m yr^{-1}. Thinning rates of 0.5 m yr^{-1} were found at elevations as high as 1700 m around 65.2°N, and this coincides with the strongest thinning observed in the radar *dH/dt* map in the upper elevations. Since it is unlikely that the magnitude of the strong thinning in the outlet glaciers could be caused by increased melting and/or reduced snowfall, *Krabill et al.* [1999] and *Abdalati et al.* [this issue] interpreted these results as being evidence of increased ice flow, possibly caused by an increase in surface meltwater reaching the ice sheet bed and reducing basal friction. Depending upon the time frame of when this change may have occurred, it is possible that some or even all of the thinning in the upper elevations east of the ice divide may be the result of increased ice flow.

Thomas et al. [2000] measured horizontal surface velocities using GPS along the 2000-m contour in southern Greenland spaced roughly every 30 km. The GPS observations east of the ice divide were, on average, around 2500 m in elevation because of crevasses and/or nunataks at the lower elevations. The downward surface velocity due to ice flow is simply the product of the horizontal surface velocity and the surface slope. This downward component to the overall rate of elevation change is offset by the accumulation rate and the product of the vertical strain rate and ice sheet thickness [*Bolzan et al.*, 1995]. A plot of the downward velocity due to ice flow for the GPS sites east and west of the ice divide is shown in Figure 6. The region in the east between 67° and 69° N was excluded because of the presence of a local ice dome. Estimates for the local slope were obtained from a digital elevation model (DEM) derived from various remote sensing data sets (satellite and airborne altimetry) [*Bamber et al.*, 2001].

The results show several interesting features. First, while the average downward velocity is nearly the same in the east (0.62 m yr^{-1}) and west (0.57 m yr^{-1}), the 1 SD variability in the east is 0.80 m yr^{-1} and is twice that of the variability in the west (0.39 m yr^{-1}). This is due to the substantial variability south of 67°N in the east where the effect of ice flow due to the outlet glaciers farther downstream is highly spatially variable. North of 69°N in the east, the downward velocities from ice flow are, averaging over 1° of latitude, smaller than all other areas of similar size in the east or west within the study area. Most important, it appears that the east coast outlet glaciers, south of 67°N, have a much greater effect on the downward velocities in the upper elevations than the Jakobshavn Glacier in the west, which is the fastest flowing glacier in the world. The downward velocities in the east at approximately 62.5°, 63°, 64.5°, and 65.2°N all exceed the largest downward velocity in the west (69°N), which corresponds to the Jakobshavn Glacier. Three of these exceed the downward velocity associated with Jakobshavn Glacier by >50%, with the largest (64.5°N) exceeding by >100%.

Given the results in the preceding paragraph, it is worth investigating whether or not the ice flow velocities in the

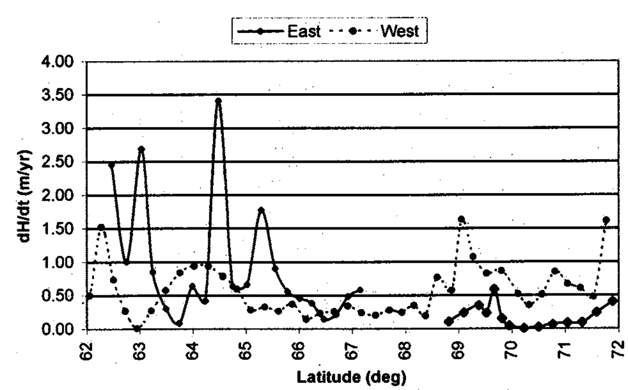

Figure 6. Estimates of the downward movement of the surface computed from measured horizontal surface velocities and ice sheet slope at locations near the 2000-m contour in the west and the 2500-m contour in the east.

southeast are consistent or inconsistent with those predicted by ice sheet geometry and net mass balance. Following the approach by *Bamber et al.* [2000], a two dimensional finite difference scheme was used to estimate horizontal balance velocities for the ice sheet. The balance velocity is the depth-averaged velocity necessary to maintain the ice sheet in steady state assuming that it is in balance. Three input data sets are required to estimate a balance velocity: surface slope, ice thickness, and net surface mass balance. A DEM derived from various satellite radar and airborne laser altimeter surveys [*Bamber et al.*, 2001] was used to obtain the surface slope data. The ice thickness data were obtained from an improved compilation of older measurements along with the recent PARCA ice thickness data [*Bamber et al.*, this issue]. The net surface mass balance was estimated using a recently published compilation [*Jung-Rothenhausler et al.*, 2000] of accumulation minus ablation, which was calculated using a positive degree day model [*Bamber et al.*, 2001]. A three-dimensional thermomechanical model of the ice sheet was used to obtain an estimate for the ratio of the surface to depth-averaged (balance) velocity at each location [*Bamber et al.*, 2001]. The velocity ratio is primarily dependent on the temperature profile in the ice, and for the GPS station locations it varied between 0.9 and 0.95. The velocity ratio is needed to translate the balance velocities to the surface for meaningful comparison with the GPS-measured velocities. A comparison between the balance velocities (translated to the surface) and those measured at each GPS station is shown in Figure 7.

West of the ice divide, the overall agreement is excellent between the balance and measured velocities, with a correlation coefficient of 0.90. The average and standard deviation of the differences (balance minus measured) was 0 ± 19 m yr^{-1}. There are only two areas of significant disagreement, defined here to be points where the differences exceeded 2 standard deviations. At 62.3°N the balance velocity was about 50 m yr^{-1} larger than the measured velocity at only that point. In the Jakobshavn catchment basin (69°N) the balance velocity is 50 m yr^{-1} smaller at one point but is 45 m yr^{-1} larger at an adjacent point. Thus the measured velocities in this area show a more clearly defined flow feature, but the net ice flux through this area is not significantly different than that predicted by the balance velocities. Thus, with the exception of one point at 62.3°N, the excellent agreement between the balance velocities and the measured velocities indicates that ice sheet flow west of the ice divide is consistent with long-term surface mass balance estimates.

East of the ice divide, the balance and measured velocities follow similar trends and are highly variable spatially. The correlation coefficient between the two is 0.89, nearly identical to that west of the ice divide. The average and standard deviation of the differences (balance minus model) is –20 ± 23 m yr^{-1}. The standard deviation is consistent with that west of the ice divide (SD = 19 m yr^{-1}). As seen in Figure 7b, the –20 m yr^{-1} average difference occurs because the balance velocities significantly underestimate the measured velocities in many areas. Note that the –20 m yr^{-1} is not a systematic bias, as there is good agreement north of 70°N and at many locations between major flow features south of 70° N (e.g., 63.5°, 64.2°, 66.5°, 68.8°N). However, significant (> 2 SD) differences occur in the areas around 63.0° N, 64.5° N, and 65.3° N, where the balance velocities are 50-90 m yr^{-1} smaller than the measured velocities. In addition, the area between 69° and 70°N has balance velocities that are consistently smaller than the measured velocities and differ by large amounts on a percentage basis. Considering these results and the corresponding large downward velocities in Figure 6, we cannot rule out the possibility that increased ice flow in the lower elevations has migrated farther upstream and is now affecting the long-term mass balance in these areas. If true, this has important implications for assessing the impact of climate change on the Greenland ice sheet and its corresponding influence on sea level rise.

Certainly, there is need for further study and analysis of this issue. A key area identified for future PARCA research is an outlet glacier program to identify and quantify the processes controlling glacier motion and the sensitivity of glacier speed to changes in these processes [*Thomas and the PARCA Investigators*, this issue]. We believe that further study of the potential impact of increased outlet glacier flow on the upper elevations of the southeastern area of the Greenland ice sheet is warranted. In addition, multidecadal time series of elevation change estimates for the upper elevations of the ice sheet will be required to definitively determine whether or not the thinning east of the ice divide and south of 67°N is due to long-term change or decadal variations in accumulation.

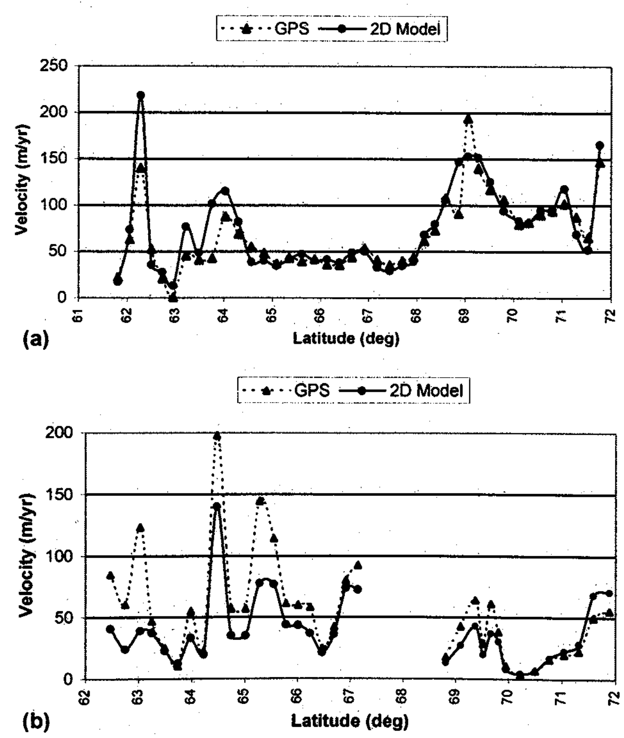

Figure 7. Measured and modeled horizontal surface velocities: (a) west of the ice divide along the 2000-m contour and (b) east of the ice divide around the 2500-m contour.

6. Conclusions

We examined the spatial pattern of elevation change estimates for the southern Greenland ice sheet derived from satellite radar altimeter data for the period from 1978 to 1988. A variety of in situ data sets collected from PARCA field investigations were used to help understand their cause(s). As reported previously, the results from 12 ice cores widely distributed in the study area indicate that much of the spatial variability in the elevation change estimates can be explained by temporal variations in accumulation. Most notably, the areas of largest thickening and thinning, east and west of the ice divide around 66°N, experienced substantial decadal fluctuations in accumulation sufficient to explain the observed elevation change rates which span the range from +24 to –24 cm yr^{-1}. Examination of the accumulation record in three deeper ice cores in the study area indicates that the decadal variability this century is consistent with that in past centuries. The results also showed that the magnitude of accumulation variability in southern Greenland is at least partially related to surface elevation, with decreasing variability as elevation increases.

Elevation change estimates in the NW of the study area around the 2000-m elevation contour were found to be inconsistent with both short- and long-term changes due to accumulation fluctuations. In addition, significant disagreement with laser altimeter elevation change estimates for the period of 1993-1998 were also found which could not be explained by accumulation changes. Examination of the stratigraphy in several shallow ice cores in the NW found that 1977 and 1978 were years of significant melting in this area which were followed by many years of very little melt activity. This likely resulted in a significant downward bias in the 1978-1988 elevation change estimates in this area which would be dependent on the spatial variability in melt intensity and therefore on elevation. The radar elevation change estimates in this area were corrected using a linear correction dependent on surface elevation.

Examination of measured surface velocities found that the contribution from ice flow to the downward movement of the surface is substantially larger in several southeastern areas than anywhere else in the study area, including the area upstream of Jakobshavn Glacier. Comparison of the measured surface velocities with those calculated assuming steady state balance showed very good agreement overall, but there were many instances in the southeast where the steady state velocities were significantly smaller than measured surface velocities. On the basis of these results, we cannot rule out the possibility that increased ice flow in lower-elevation outlet glaciers has migrated farther upstream and is now affecting the long-term mass balance in the southeast. Further study and analysis is needed to determine the time frame and potential impact of increased outlet glacier ice flow on the mass balance of the higher-elevation parts in southeastern Greenland.

Acknowledgments. This work was supported by the NASA Earth Science Enterprise under grants NAG5-6837 and NAG13-99014 to the University of Missouri-Columbia, grant NAG5-5031 to the University of Arizona, grant NAG5-6779 to the Desert Research Institute, and grants NAG5-5032 and NAG5-6817 to the Ohio State University (OSU). JLBs work was partially supported by the UK NERC under grant GR3/9791. The detailed visible stratigraphy for the shallow ice cores was kindly provided by Z. Li from OSU.

References

Abdalati, W., W. Krabill, E. Frederick, S. Manizade, C. Martin, J. Sonntag, R. Swift, R. Thomas, W. Wright, and J. Yungel, Outlet glacier and margin elevation changes: near-coastal thinning of the Greenland ice sheet, *J. Geophys. Res.*, this issue.

Arthern, R.J., and D.J. Wingham, The natural fluctuations of firn densification and their effect on the geodetic determination of ice sheet mass balance, *Clim. Change*, *40*, 605-624, 1998.

Bales, R.C., J.R. McConnell, E. Mosley-Thompson, and G. Lamorey, Accumulation map for the Greenland ice sheet: 1970-1990, Geophys. Res. Lett., in press, 2001.

Bamber, J.L., R.J. Hardy, and I. Joughin, An analysis of balance velocities over the Greenland ice sheet and comparison with synthetic aperture radar interferometry, *J. of Glaciol.*, *46*(152), 67-74, 2000.

Bamber, J.L., S. Ekholm, and W. Krabill, A new high-resolution digital elevation model of Greenland fully validated with airborne laser altimeter data, *J. Geophys. Res.*, *106*, 6733-6745, 2001.

Bamber, J.L., R. Layberry, and S. Gogineni, A new ice thickness and bed data set for the Greenland ice sheet 1, measurement, data reduction, and errors, *J. Geophys. Res.*, this issue.

Bolzan, J., A glaciological determination of the mass balance in central Greenland (abstract), *Eos Trans. AGU*, *73*(43), Fall Meet. Suppl., 203, 1992.

Bolzan, J., and M Strobel, Accumulation rate variations in central Greenland, *J. of Glaciol.*, *40*(135), 56-66, 1994.

Bolzan, J., E. Waddington, R. Alley, and D. Meese, Constraints on Holocene ice-thickness changes in central Greenland from the GISP2 ice-core data, *Ann. Glaciol.*, *21*, 33-39, 1995.

Davis, C.H., Satellite radar altimetry, *IEEE Trans. Microwave Theory Tech.*, *40*(6), 1070-1076, 1992.

Davis, C.H., Growth of the Greenland ice sheet: A performance assessment of altimeter retracking algorithms, *IEEE Trans. Geosci. Remote Sens.*, *33*(5), 1108-1116, 1995.

Davis, C.H., Temporal change in the extinction coefficient of snow on the Greenland ice sheet from an analysis of Seasatand Geosat altimeter data, *IEEE Trans. Geosci. Remote Sens.*, *34*(5), 1066-1073, 1996.

Davis, C.H., A robust threshold retracking algorithm for measuring ice sheet surface elevation change from satellite radar altimeters, *IEEE Trans. Geosci. Remote Sens.*, *35*(4), 974-979, 1997.

Davis, C.H., and H.J. Zwally, Geographic and seasonal variations in the surface properties of the ice sheets by satellite radar altimetry, *J. Glaciol.*, *39*(133), 687-697, 1993.

Davis, C.H., C.A. Kluever, and B.J. Haines, Elevation change of the southern Greenland ice sheet, *Science*, *279*, 2086-2088, 1998.

Davis, C.H., C. A. Kluever, B.J. Haines, C. Perez, and Y.T. Yoon, Improved elevation change measurement of the southern Greenland ice sheet from satellite radar altimetry, *IEEE Trans. Geosci. Remote Sens.*, *38*(3), 1367-1378, 2000.

Douglas, B.C., R.E. Cheney, L. Miller, and R.W. Agreen, Greenland ice sheet: Is it growing or shrinking, *Science*, *248*, 288, 1990.

Drew, A.J., Glacial movements in Greenland from Doppler satellite observations, *Inst. Polar Stud. Rep. 82*, Ohio State Univ., Columbus, 1983.

Frich, P., et al., North Atlantic Climatological Data set (NACD Version 1) - Final report, Dan. Meteorol. Inst., Copenhagen, 1996.

Jung-Rothenhausler, F., et al., Greenland accumulation distribution: A GIS-based approach, *J. Glaciol.*, in press, 2001.

Krabill, W., R. Thomas, K. Jezek, K. Kuivinen, and S. Manizade, Greenland ice sheet thickness changes measured by laser altimetry, *Geophys. Res. Lett.*, *22*(17), 2341-2344, 1995.

Krabill, W., E. Frederick, S. Manizade, C. Martin, J. Sonntag, R. Swift, R. Thomas, W. Wright, and J. Yungel, Rapid thinning of parts of the southern Greenland ice sheet, *Science*, *283*, 1522-1524, 1999.

Krabill, W., W. Abdalati, E. Frederick, S. Manizade, C. Martin, J. Sonntag, R. Swift, R. Thomas, W. Wright, and J. Yungel, Greenland ice sheet: High-elevation balance and peripheral thinning, *Science*, *289*, 428-430, 2000.

Legresy, B., F. Remy, and P. Vincent, Is the south Greenland dome moving westward?, paper presented at XXV General Assembly, Eur. Geophys. Soc., Nice, France, April 25-29, 2000.

McConnell, J.R., R.J. Arthern, E. Mosley-Thompson, C.H. Davis, R.C. Bales, R. Thomas, J.F. Burkhart, and J.D. Kyne, Greenland ice sheet elevation changes derived from measured snow accumulation, *Nature*, *406*, 877-879, 2000.

McConnell, J.R., G. Lamorey, E. Hanna, E. Mosley-Thompson, R. Bales, D. Belle-Oudry, and J.D. Kyne, Annual net snow accumulation over southern Greenland from 1975 to 1998, *J. Geophys. Res.*, this issue.

Mosley-Thompson, E., J.R. McConnell, R.C. Bales, Z. Li, P-N. Lin, K. Steffen, L.G. Thompson, R. Edwards and D. Bathke, Local to regional-scale variability of annual net accumulation on the Greenland ice sheet from PARCA cores, *J. Geophys. Res.*, this issue.

Ridley, J.K., and K.C. Partington, A model of satellite radar altimeter return from the ice sheets, *Int. J. Remote Sens.*, *9*(4), 601-624, 1988.

Tapley, B.D., et al., The Joint Gravity Model 3, *J. Geophys. Res.*, *101*, 28,029-28,049, 1996.

Thomas, R.H. and the PARCA Investigators, Program for Arctic Regional Climate Assessment (PARCA): Goals, key findings, and future directions, *J. Geophys. Res.*, this issue.

Thomas, R.H., C.H. Davis, E. Fredrick, S. Manizade, W. Krabill, J. McConnell, and J. Sonntag, Greenland ice sheet elevation change since 1978 from radar and laser altimetry, *Polar Geogr.*, *23*(3), 169-184, 1999.

Thomas, R., T. Akins, B. Csatho, M. Fahnestock, P. Gogineni, C. Kim, and J. Sonntag, Mass balance of the Greenland ice sheet at high elevations, *Science*, *289*, 426-428, 2000.

Thomas, R.H., B. Csatho, C. Davis, C. Kim, W. Krabill, S. Manizade, J. McConnell, J. Sonntag, and H.J. Zwally, Mass balance of the higher-elevation parts of the Greenland ice sheet, *J. Geophys. Res.*, this issue.

van der Veen, C.J., Interpretation of short-term ice sheet elevation changes inferred from satellite altimetry, *Clim. Change*, *23*, 383-405, 1993.

Wingham, D.J., A.J. Ridout, R. Scharroo, R.J. Arthern, and C.K. Shum, Antarctic elevation change from 1992 to 1996, *Science*, *282*, 456-58, 1998.

Yoon, Y.T., Global orbit-error analysis using stochastic filtering methods, M.S. thesis, Univ. of Mo., Columbia, 1998.

Zwally, H.J., A.C. Brenner, J.A. Major, R.A. Bindschadler, and J.G. Marsh, Growth of Greenland ice sheet: Measurement, *Science*, *246*, 1587-1589, 1989.

Zwally, H.J., Growth of Greenland ice sheet: Interpretation, *Science*, *246*, 1589-1591, 1989.

J. L. Bamber, Bristol Glaciology Centre, School of Geographical Sciences, University of Bristol, University Road, Bristol, BS8 1SS, England, UK. (j.l.bamber@bristol.ac.uk)

J. Bolzan, 354 Westview Avenue, Columbus, OH 43214. (j.bolzan@worldnet.att.net)

C. H. Davis, Department of Electrical Engineering, 323 EBW, University of Missouri-Columbia, Columbia, MO 65211. (DavisCH@missouri.edu)

J.R. McConnell, Desert Research Institute, University and Community College System of Nevada, Reno, NV 89512. (jmcconn@dri.edu)

E. Mosley-Thompson, Byrd Polar Research Center and Department of Geography, The Ohio State University, Columbus, OH 43210. (thompson.4@osu.edu)

R. H. Thomas, EG&G Services, NASA Wallops Flight Facility, Wallops Island, VA 23337. (robert_thomas@hotmail.com)

(Received July 31, 2000; revised February 7, 2001;
accepted February 15, 2001.)